Drug Development and Industrial Pharmacy, 2011; 37(5): 526–537

ISSN 0363-9045 print/ISSN 1520-5762 online
DOI: 10.3109/03639045.2010.527983

informa
healthcare

RESEARCH ARTICLE

Oral solid compritol 888 ATO nanosuspension of simvastatin: optimization and biodistribution studies

Mayank Shah[1], Krishna Chuttani[2], A.K. Mishra[2], and Kamla Pathak[1]

[1]Rajiv Academy for Pharmacy, P.O. Chhattikara, Mathura, Uttar Pradesh, India, and [2]Department of Radio Pharmaceuticals, Institute of Nuclear Medicine and Allied Sciences, Delhi, India

Abstract

The purpose of the present investigation was to develop solid lipid nanoparticles (SLNs) of simvastatin in order to enhance its oral bioavailability by minimizing its first-pass metabolism. To achieve our goal, SLNs were prepared by solvent injection technique and optimized by 2^3 full factorial experimental design using Design Expert software. The SLN formulations were optimized for amount of compritol, concentration of poloxamer, and volume of acetone in order to achieve desired responses of particle size, entrapment efficiency (EE), and cumulative drug release (CDR). Response surface plots were constructed to study the influence of each variable on each response and the interactions between any two variables were also analyzed. Formulation F_{10} with particle size of 271.18 nm, % EE of 68.16% and % CDR of 76.23%, and highest desirability value of 0.645 was selected as optimized formulation. The optimized formulation was evaluated for biodistribution and pharmacokinetics by technetium-99m (Tc-99m) radiolabeling technique in mice. The relative bioavailability of simvastatin from optimized SLNs was found to be 220%, substantiating the protective action of SLNs against liver metabolism. However, though the drug initially bypassed the liver metabolism, simvastatin continuously entered in liver to exert its therapeutic action that was evidenced by biodistribution study.

Keywords: Simvastatin; compritol 888 ATO; solid lipid nanoparticles; response surface plots; bioavailability; biodistribution

Introduction

Simvastatin, a HMG CoA reductase inhibitor, is widely used to lower blood cholesterol level. However, this drug is associated with certain drawbacks like low oral bioavailability (5%) due to extensive hepatic first-pass metabolism (Goodman and Gilman's, 2006) and susceptibility to hydrolytic degradation in gastrointestinal (GI) tract (Vanderbast et al., 2007). Cytochrome P450 3A4 system is responsible for its degradation in liver. To overcome hepatic first-pass metabolism and to enhance bioavailability, intestinal lymphatic transport of the drug can be exploited that can be possibly done by using lipids as drug carrier (Nishioka and Yoshino, 2001). Lipids can enhance lymph formation and simultaneously promote lymph flow rate. Transport of drugs through the intestinal lymphatics via the thoracic lymph duct to the systemic circulation at the junction of the jugular and left subclavian vein avoids presystemic hepatic metabolism and therefore enhances bioavailability (Suresh et al., 2007).

Amongst the lipid-based drug-delivery system, we have selected solid lipid nanoparticles (SLNs). SLNs introduced in 1991 represent an alternative carrier system to traditional colloidal carriers, such as emulsions, liposomes, and polymeric micro- and nanoparticles (Müller et al., 2000). They combine the advantages of colloidal lipid emulsions with advantages of particles with a solid matrix. Compared with colloidal carriers, SLNs are more preferred because they offers certain advantages such as good tolerability, lower cytotoxicity (Maaßen et al., 1993; Muller et al., 1996), higher bioavailability by oral administration (Yang et al., 1999), increase in the drug stability (Mehnert and Mäder, 2001), biodegradability, and cost effectiveness (Mukherjee et al.,

Address for Correspondence: Kamla Pathak, Department of Pharmaceutics, Rajiv Academy for Pharmacy, National Highway #2, P.O. Chhattikara, Mathura–281001, Uttar Pradesh, India. Tel.: +91-565-2913018. Fax: +91-565-2825050. E-mail: kamla_rap@yahoo.co.in

(Received 21 June 2010; revised 16 September 2010; accepted 24 September 2010)

2007). Consisting of physiological and biodegradable lipids, lipid nanoparticles are suitable for the incorporation of lipophilic, hydrophilic, and poorly water-soluble drugs within the lipid matrix in considerable amounts (Almeida et al., 1997). Aqueous dispersions of SLN are preferred with regard to the ease of handling (no reconstitution necessary) and for cost reasons (Freitas and Muller, 1998).

Simvastatin, a poor bioavailable drug, has been researched for improvement in bioavailability and therapeutic efficacy by various approaches including nanoparticulate formulations. Ali et al. (2010) have reported anticancer effects of simvastatin–tocotrienol lipid nanoparticles. The entrapment of simvastatin in the oily nanocompartments formed by tocotrienol inclusion into the solid matrix of the nanoparticles resulted in an initial burst release of ~20% in 10 h followed by a plateau. The antiproliferative effects on malignant + SA mammary epithelial cells confirmed the potency of the combined treatment. Margulis-Goshen and Magdassi (2009) have reported formation of simvastatin nanoparticles from microemulsion wherein the microemulsion containing a volatile solvent as an oil phase is converted into nanoparticles in the form of dry non-oily flakes by freeze-drying. The freeze-dried flakes contained >95% of the drug as amorphous particles smaller than 100 nm. The tablets containing the flakes of simvastatin nanoparticles showed tremendous enhancement in dissolution profile compared with conventional tablets but the major problem was simvastatin nanoparticles were initially amorphous, but a slow crystallization process took place when the product was stored at room temperature. Moreover, the process does not appears be cost-effective. Hence, the aim of our study was to develop a simple, cost-effective nanosized formulation of simvastatin utilizing lipid carrier by simple solvent injection technique. Compritol 888 ATO was selected as the lipidic carrier because of its favorable attributes of its nonpolarity and low cytotoxicity than other lipids like dynasan, cetyl palmitate, solid paraffin, stearic acid, beeswax, and so on (Nastruzzi, 2005). Moreover, it provides high drug entrapment efficiency (EE) as the presence of high amount of mono-, di-, and triglycerides in compritol help the drug to solubilize in the lipid fraction and the less-defined mixture of acylglycerol provides additional space for drug molecules to get entrapped (Manjunath et al., 2005). Optimization studies for the development of nanoparticulate formulation of simvastatin were done by 2^3 full factorial experimental design and the data analyzed using Design Expert 7.1.1® software (Stat-Ease, Inc., Minneapolis, MN). The second part of this study is associated with *in vivo* evaluation of simvastatin SLNs for its pharmacokinetic and biodistribution by radiolabeling with technetium-99m (Tc-99m).

Experiments and methods

Materials

Simvastatin was kind gift of Ranbaxy Laboratories, India. Compritol 888 ATO was kind gift of Gatteffose, France. Poloxamer 407 was purchased from BASF Mount Olive, NJ). Dialysis bag was supplied from Hicon Media, Mumbai, India. Tc-99m was generously supplied by regional center for radio-pharmaceutical, BRIT, Delhi, India. Mice were obtained from NICD, New Delhi, India. Stannous chloride was obtained from Sigma Chemicals, St. Louis, MO. Other chemicals are of analytical grade.

Methods

Experimental design

In this study, a 2^3 full factorial experimental design was used to optimize SLNs. The amount of compritol (X_1), concentration of poloxamer 407 (X_2), and volume of acetone (X_3) were selected as independent variables. Each factor was set at a high level and low level and eight formulations of SLNs (F_1 to F_8) were prepared according to the design as shown in Table 1. The particle size, % EE, and % cumulative drug release (CDR) were taken as response parameters.

Preparation of SLNs

SLNs were prepared by solvent injection technique. Simvastatin (15 mg) and specified amount of compritol was dissolved in specified volume of acetone with gentle stirring. The resulting solution was rapidly injected into the 10 mL of aqueous phase containing specified amount of poloxamer 407 that was kept at room temperature and continuously stirred at 400 rpm for 30 min on a magnetic stirrer. The 0.1 N HCl (4 mL) was added to the dispersion to decrease the pH to

Table 1. The 2^3 full factorial design for formulation of solid lipid nanoparticles of simvastatin and the response parameters.

Formulation code	Amount of compritol (X1)	Concentration of poloxamer 407 (X2)	Volume of acetone (X3)	Particle size (nm)	% EE	% CDR
F_1	−1	−1	−1	311.7	71.41	61.13
F_2	−1	−1	+1	293.8	63.89	73.94
F_3	−1	+1	−1	236.1	56.62	82.69
F_4	−1	+1	+1	226.8	49.37	86.58
F_5	+1	−1	−1	369.2	79.61	46.6
F_6	+1	−1	+1	330.5	72.83	53.71
F_7	+1	+1	−1	294.4	69.38	61.24
F_8	+1	+1	+1	277.5	59.06	68.43

(X1: −1 = 200 mg, +1 = 400 mg; X2: −1 = 0.8%, +1 = 1.2%; X3: −1 = 1 mL, +1 = 2 mL).

around 1.5 to 2 to cause the aggregation of SLNs for the ease of separation. Thereafter, the dispersion was centrifuged to 10,000 rpm for 30 min at 10°C in Remi cooling centrifuge (Model C-24BL, VCAO-779, Vasai, India), purified by dialysis (Shah and Pathak, 2010) and resuspended in 10 mL distilled water containing 4% poloxamer 407 (by weight) as stabilizer with stirring at 1000 rpm for 10 min.

Particle size determination

The particle size of the formulations was determined by laser scattering technique using Malvern Hydro 2000SM (Malvern Instruments, UK) after appropriate dilution with double-distilled water. Light scattering was measured at an angle of 90°. The aqueous nanoparticulate dispersion was added to the sample dispersion unit containing stirrer and then stirred to minimize the interparticle interactions while the laser obscuration range was maintained between 10% and 20%.

Entrapment efficiency

The EE was calculated by Equation (1):

$$EE = [Wa - (Ws + Wp)]/Wa \times 100 \quad (1)$$

where W_a is the amount of drug added in system; W_s is the amount of drug in supernatant after the centrifugation; and W_p is the amount of drug in the purification medium. The amounts were calculated from concentration values obtained from calibration curve on spectrophotometric analysis of the samples at 239 nm (Shimadzu Pharmaspec 1700, Kyoto, Japan).

In vitro drug release

In vitro drug release study of SLNs was performed by dialysis bag diffusion technique. Solid lipid nanosuspension equivalent to 5 mg simvastatin was filled in dialysis bag (MWCO 12–14 kDa) and immersed in a receptor compartment containing 150 mL of phosphate buffer pH 7.4 that was stirred at 100 rpm and maintained at a temperature at 37 ± 0.5°C. The receptor compartment was covered to prevent evaporation of dissolution medium. Five milliliters of samples were withdrawn at various time intervals and replaced with fresh media. The samples were appropriately diluted and the absorbance was measured at 239 nm. The absorbance was used to calculate concentration using calibration curve.

Analysis of responses by Design Expert

Design Expert 7.1.1., USA was used for the analysis of effect of each variable on the designated responses. Quantitative and qualitative contribution of each variable on each of the response was analyzed. The significant response polynomial equations generated were used to validate the statistical design (Bolton and Bon, 2004). Response surface plots were generated to visualize simultaneous effect of each variable on each response parameter and the possible interactions between X_1X_2, X_2X_3, and X_1X_3 were also studied.

Selection of optimized formulation

Optimized formulation (F_{10}) was selected on the basis of small particle size, high EE, *in vitro* CDR after 55 h and with good desirability.

Transmission electron microscopy

The optimized SLNs were visualized by TEM (Hitachi 500, Tokyo, Japan). The samples were diluted 20 times and stained with 2% w/v phosphotungstic acid. After 30 sec, samples were washed with ultrapurified water and excess fluid was removed using filter paper. Finally, the sample was placed on copper grids with films for viewing.

In vivo evaluation

Radiolabeling of simvastatin suspension and optimized simvastatin SLNs was done by direct method using stannous chloride as reducing agent (Babbar et al., 1991). In brief, 1 mL of simvastatin suspension and 1 mL of simvastatin SLNs was mixed individually with stannous chloride. To adjust the pH of this mixture, 10 µL of sodium hydrogen carbonate solution was added. Then 0.1 mL of freshly eluted Tc-99m (2 mCi) was added to each preparation, mixed well, and incubated at room temperature. Final radioactivity present in the preparation was checked using gamma-ray counter (Capintech, CAPRAC–R, Ramsey, NJ). The amount of stannous chloride, pH of the final preparation, and incubation time should be optimized previously.

The effect of the amount of stannous chloride, the final pH of the preparation, and the incubation time on labeling efficiency was optimized by changing one parameter at a time and by performing quality control tests for the labeled complex (Theobald, 1990). For optimizing amount of stannous chloride, a range of 25 to 400 µg of stannous chloride was used. Similarly, pH of the reaction mixture was varied from 4 to 7 and incubation time was varied between 5 and 30 min.

The labeling efficiency of simvastatin suspension and simvastatin SLNs was determined by developing ascending thin-layer chromatography (TLC) using instant TLC (ITLC) strips coated with silica gel (Gelman Science Inc., Ann Arbor, MI). The ITLC strips were used to determine free technetium and percentage of radiocolloids in the preparation. ITLC strips were spotted with 1 to 2 µL of labeled complex at 1 cm above the bottom. These strips were developed using acetone and a solvent system to determine free Tc-99m pertechnetate and reduced/hydrolyzed (R/H) Tc-99m. The solvent front was allowed to reach to a height of approximately 6 to 8 cm from the origin and the strip was cut horizontally into two halves. Radioactivity in each half was determined by well-type gamma-ray spectrometer. The free pertechnetate present in the preparation migrates to the top portion of the ITLC strip, leaving

the radiocolloids (reduced/hydrolyzed technetium) along with the labeled complex at the point of application. The presence of radiocolloids was determined by developing ITLC strip using pyridine:acetic acid:water in ratio of 3:5:1.5. Reduced/hydrolyzed Tc-99m present in the preparation will remain at point of application, while both the free Tc-99m-pertechnetate and labeled complex migrate with the solvent front. Thus ITLC strips were used to determine free Tc-99m and reduced/hydrolyzed technetium, and based on these two parameters labeling efficiency was determined (Mishra et al., 1991).

All surgical and experimental procedures were reviewed and approved by the animal and ethics review committee of Rajiv Academy for Pharmacy, Mathura, India. Euthanasia and disposal of carcass was in accordance with the ethical committee guidelines. Swiss albino mice (25 ± 5 g) were used for pharmacokinetic and biodistribution studies. Before experimentation, they were divided in two groups with each group containing 21 mice. The mice were fasted for 12 h before the experiments but had free access to water. The radiolabeled simvastatin suspension and optimized SLNs with final radioactivity of 2 mCi/mL was prepared and were separately administered to each mouse in a dose of 5 mg/kg using cannula (16 # gauge). The remaining suspension was labeled as standard. Group 1 received simvastatin suspension and group 2 received SLN of simvastatin.

For pharmacokinetic evaluation, the mice ($n = 3$) were anesthetized using chloroform at 0.5, 1, 2, 4, 6, 24, and 48 h post-administration and blood was collected via cardiac puncture. Blood samples were transferred into preweighed test tubes and reweighed. The samples were analyzed for radioactivity by gamma-ray counter. Radioactivity in various samples was determined in the unit of counts. Along with the blood samples, the standard solution was also checked for its radioactivity that accounted to standard counts. From this data, percent activity/gram (% A/G) was calculated by using Equation (2).

$$\%\ \text{A/G} = [(\text{counts/weight})/\text{standard counts}] \times 100 \quad (2)$$

Area under the curve (AUC), relative bioavailability, elimination half-life, volume of distribution, and other pharmacokinetic parameters were calculated using QuickCal software (developed by Dr. Shivaprakash, Plexus, Ahmedabad, India).

After collecting blood at the end of each time points (0.5, 1, 2, 4, 6, 24, and 48 h), each mice was sacrificed humanly and various organs including the heart, liver, lungs, kidneys, spleen, stomach, and intestine were then isolated. Each organ was weighed and radioactivity was determined using gamma-ray counter.

Results and discussion

Each SLN formulation of the experimental design was evaluated for particle size, % EE, and % CDR after 55 h and the results are tabulated in Table 1. The response parameters were analyzed using Design Expert software that provided considerable useful information and reaffirmed the utility of statistical design for conduct of experiments. The selected independent variables like the amount of compritol 888 ATO, concentration of poloxamer 407, and volume of acetone significantly influenced the particle size, % EE, and % CDR that is very much evident from the results in Table 1. The *in vitro* drug release profiles of F_1 to F_8 (Figure 1) exhibit an initial fast release till 10 h followed by a relatively slow almost constant release for the next 45 h. The release pattern is quite similar to the release pattern reported by other researchers (Zhang et al., 2003; Derakhshandeh et al., 2007). As evident formulation F_4 formulated using low levels of compritol and high levels of both poloxamer and acetone displayed highest % CDR that was quite in contrast to formulation F_5 formulated with high levels of compritol and low levels of both poloxamer and acetone that exhibited least % CDR. The results are directly correlatable to particle size as F_4 with least particle size of 226.8 nm offered more surface area for dissolution, whereas F_5 with maximum nanometric particle size of 369.2 nm offered smaller surface area for dissolution. Correspondingly, %CDR at 55 h was highest for F4 and least for F5.

To validate the experimental design using a polynomial equation, all the response parameters were selected. A two-level experimental design provides sufficient data to

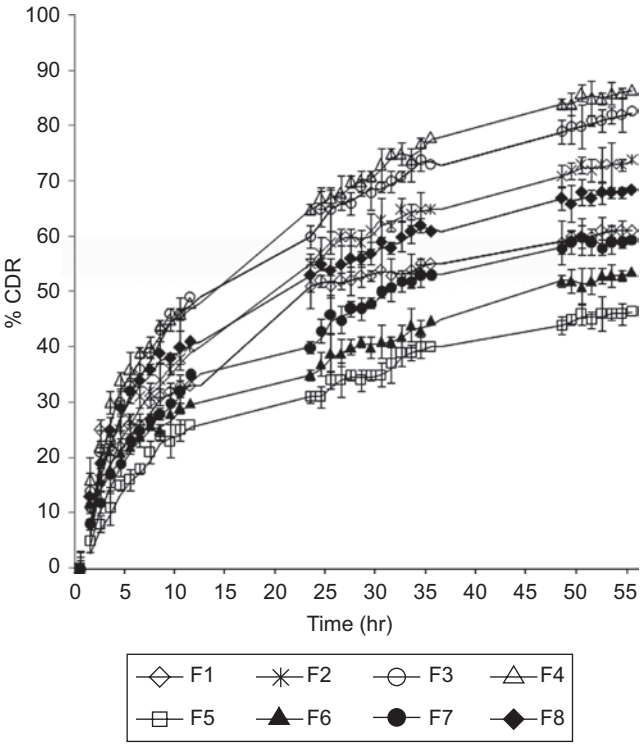

Figure 1. *In vitro* drug release profiles solid lipid nanoparticles of simvastatin (◇) F_1, (✳) F_2, (○) F_3, (△) F_4, (□) F_5, (▲) F_6, (●) F_7, and (◆) F_8 in phosphate buffer pH 7.4 using dialysis bag (MWCO 12–14 kDa).

fit a polynomial equation, hence the response polynomial coefficients were determined in order to evaluate each response. Each response coefficient was studied for its statistical significance at 95% level confidence level and nonsignificant response coefficients were removed to generate significant polynomial response Equations (3)–(6) for particle size, % EE, and % CDR.

$$\text{Particle size (nm)} = 292.5 + 25.4X_1 - 33.8X_2 - 10.35X_3 + 1.85X_1X_2 - 3.55X_1X_3 - 3.8X_2X_3 + 1.66X_1X_2X_3 \quad (3)$$

$$\%\ \text{EE} = 65.37 + 4.73X_1 - 6.7X_2 - 3.97X_3 - 0.42X_1X_2X_3 \quad (4)$$

$$\%\ \text{CDR} = 66.96 - 8.83X_1 + 7.87X_2 + 3.82X_3 + 0.84X_2X_3 + 1.38X_1X_2X_3 \quad (5)$$

These equations were utilized for validation of the experimental design. An extra design checkpoint formulation (F_9) was prepared and the predicted value(s) for particle size, % EE, and % CDR were generated using Design Expert software. Experimental values were determined by formulating and evaluating F_9 and close resemblance between predicted and experimental values indicated validity of the generated model (Table 2).

The possible interactions between X_1X_2, X_2X_3, and X_1X_3 for each response were studied (Figure 2). Graphically, the interactions are visualized by lack of parallelism in the lines but in our case parallel lines obtained for each interaction term(s) for each response parameter(s) indicated lack of interactions that in turn indicated that the experimental design has maximum efficiency in estimating main effects (Bolton and Bon, 2004). The response surface plots (Figure 3) generated using polynomial equations represent simultaneous effect of any two variables on response parameter taking one variable at constant level. On careful observation, the qualitative effect of each variable on each response parameter can be visualized. However, the Design Expert can analyze both qualitative and quantitative effect of variables on response parameters as shown in Figure 4. Here the positive sign indicates that the increase in level of one variable causes increase in the respective response parameter, whereas negative sign indicates that the increase in level of one variable causes decrease in response parameter.

Thus an increase in the amount of compritol caused an increase in particle size. The fact that the size of lipid nanoparticles is highly dependent on lipid concentration can be explained in terms of tendency of lipid to coalesce at high lipid concentration. According to Stokes's law, this behavior can be explained by difference in density between internal and external phase (Leroux et al., 1994). Schubert and Müller-Goymann (2003) established that an increase in particle size of SLNs was due to a reduction in the diffusion rate of the solute molecules in the outer phase as a result of viscosity increase in the lipid–solvent phase. With increasing the amount of compritol, % EE is bound to increase because of the increased concentration of mono-, di-, and triglycerides that act as solubilizing agents for highly lipophilic drug (Manjunath et al., 2005). Moreover, the increase in particle size might be due to the fact that increased amount of lipid provides additional space for drug molecules to entrap.

On the other hand, an increase in the concentration of poloxamer 407 resulted in a decrease in particle size. This might be due to the surfactant-induced reduction in surface tension between aqueous phase and organic phase used in formulation of SLNs. Additionally, the surfactant also helps in stabilizing the newly generated surfaces and prevents particle aggregation (Schubert and Müller-Goymann, 2003). Similarly, an increase in surfactant concentration resulted in decline of % EE because of the well-known fact that the aqueous solubility of drug increases with increasing concentration of surfactant in aqueous phase. However, the percent CDR increased because of the corresponding decrease in particle size that in turn increased the surface area available for dissolution. Increasing the volume of acetone also had an effect similar to that of concentration of poloxamer but to a lesser extent as can be deduced from Figure 4.

Thus both qualitative and quantitative influence of independent variables on particle size, % EE, and % CDR were clearly interpreted by Design Expert that is an equally advantageous tool for selection of optimized formulation. The tool offers the possibility to vary each variable simultaneously and presents possible optimum selections with their respective desirability value (Bhavsar et al., 2006). Thus based on our criteria of lower particle size, higher % EE, and higher % CDR after 55 h, formulation F_{10} was selected as optimized formulation (highest desirability value of 0.645). Consequently, the coded optimized level for amount of compritol, concentration of poloxamer, and volume of acetone for F_{10} were identified as −1.0, 0.57, and −1.0, respectively. These coded optimized values can be converted to actual optimized values by using principles of transformation by use of the following Equation (6).

$$\text{Coded value (X)} = \frac{\{\text{Actual value (X')} - \text{Average of the actual level}\}}{\text{1/2th difference between actual level}} \quad (6)$$

Thus for each variable, actual optimized values were calculated by the following equations.

$$\text{Amount of compritol (mg)}\ (X_1') = 50\,(X_1) + 150 \quad (7)$$

$$\text{Concentration of poloxamer 407 (\% w/v)}\ (X_2') = 0.2\,(X_2) + 1.0 \quad (8)$$

$$\text{Volume of acetone (mL)}\ (X_3') = 0.5\,(X_3) + 1.5 \quad (9)$$

Table 2. Evaluation parameters of extra design check point formulation F_9 for validation of experimental design.

Response parameters	Experimental value	Predicted value	% RSD
Particle size (nm)	276.13	292.5	4.07
% EE	61.86	65.37	3.75
% CDR	62.29	66.96	5.11

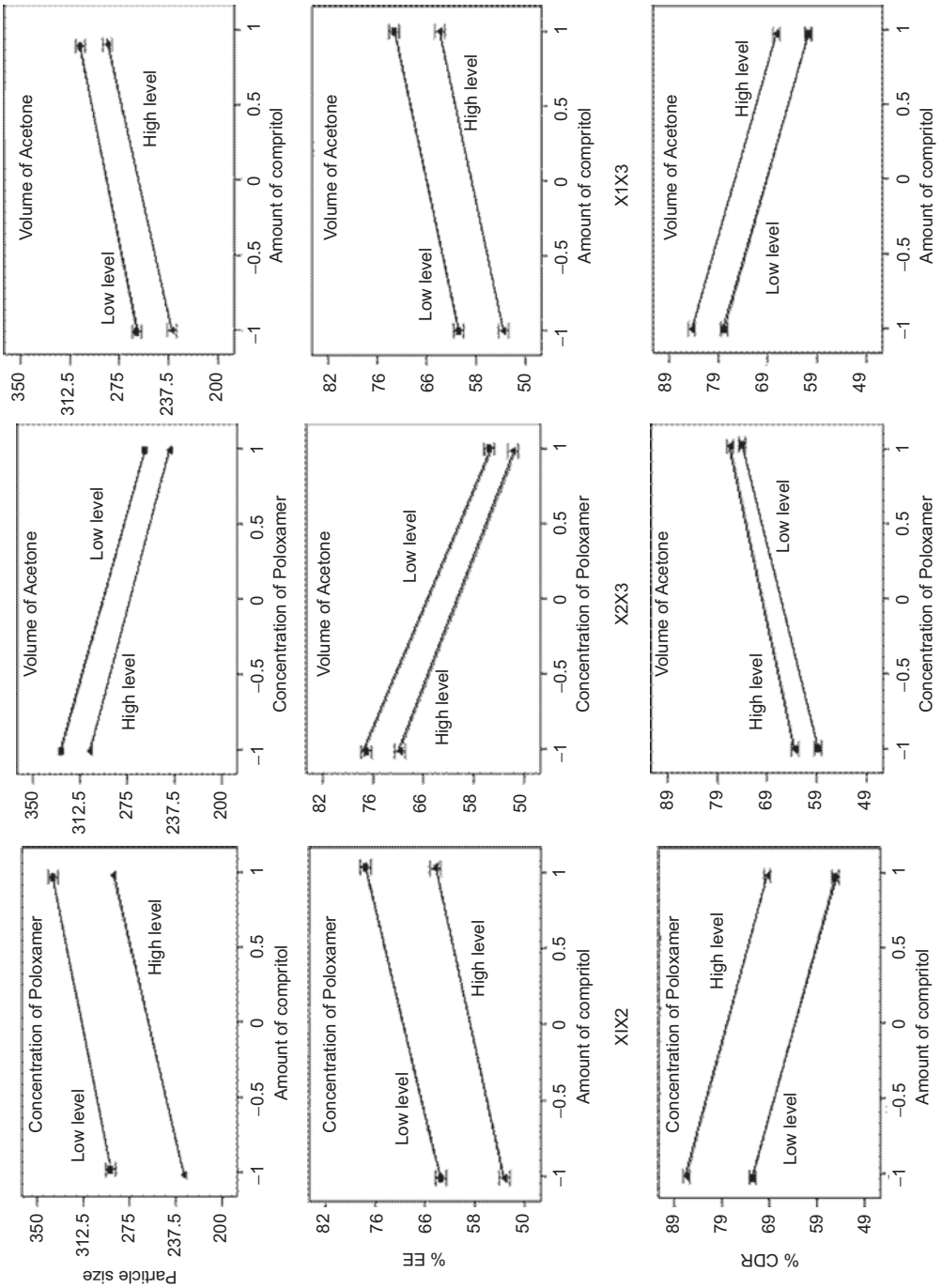

Figure 2. Interaction plots to analyze the effect of interaction between X_1X_2, X_2X_3, and X_1X_3 on (A) particle size, (B) entrapment efficiency, and (C) cumulative drug release from SLNs of simvastatin where X_1 = amount of compritol, X_2 = concentration of poloxamer 407, and X_3 = volume of acetone.

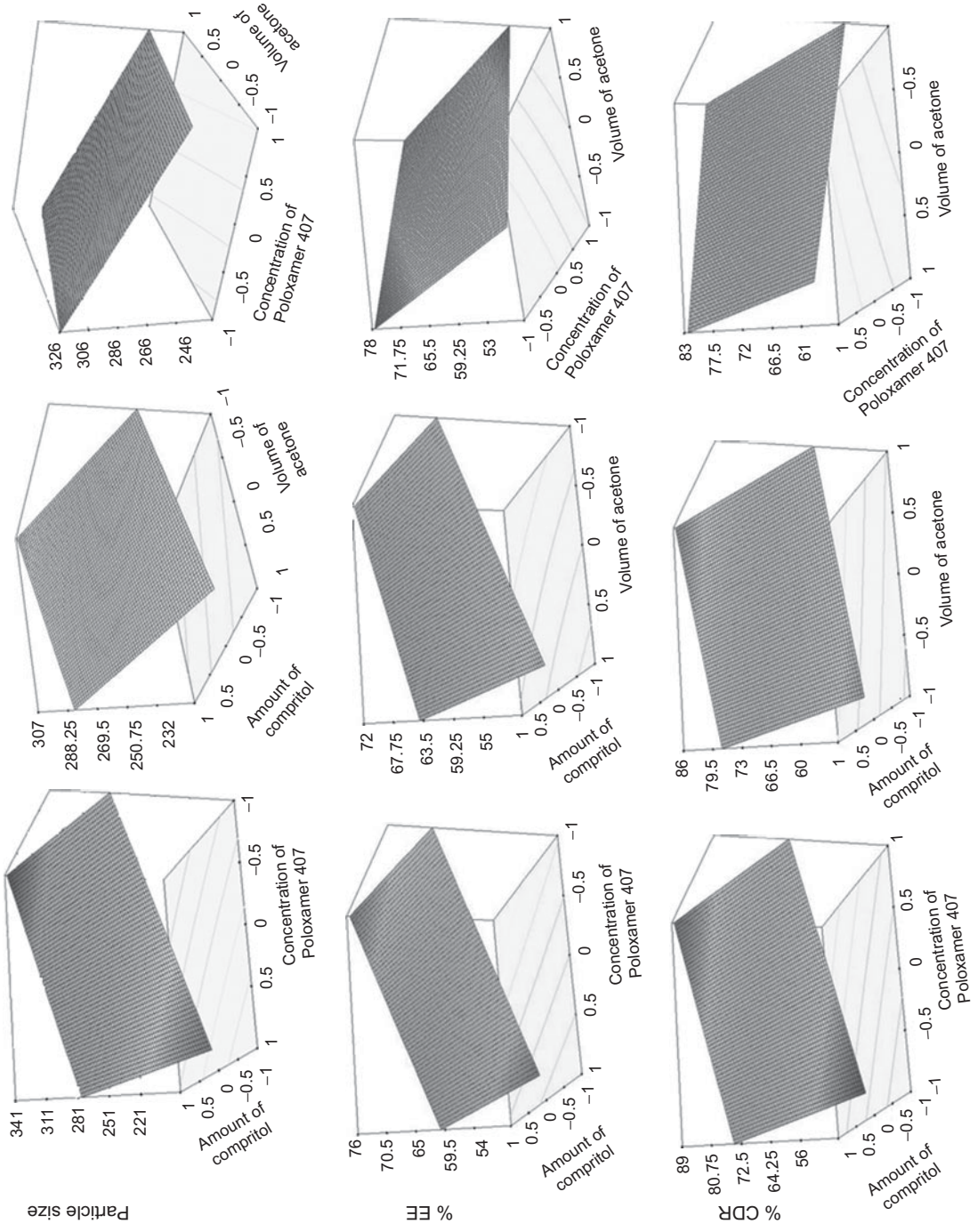

Figure 3. Response surface plots demonstrating the influence of variables on (A) particle size of SLNs, (B) entrapment efficiency of SLNs, and (C) cumulative drug release from SLNs.

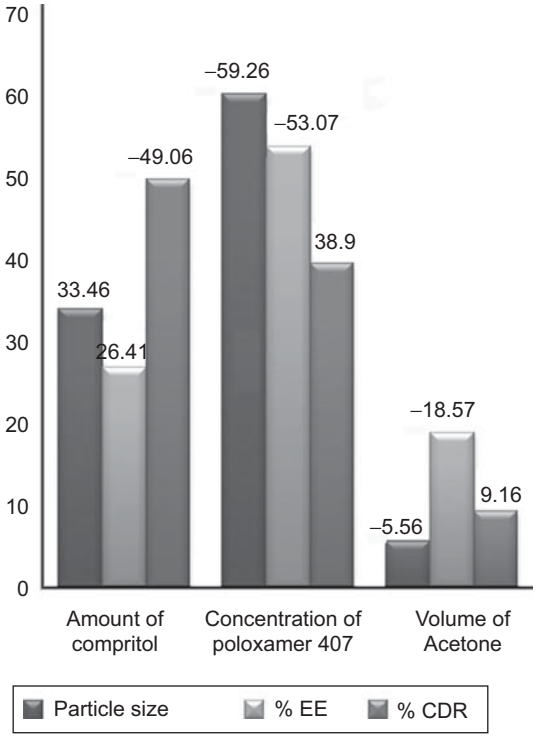

Figure 4. Percentage contribution and effect of independent variables on various response parameters of SLNs.

Thus, optimized formulation F_{10} was prepared using 100 mg of compritol, 1.1 % w/v of poloxamer, and 1 mL of acetone and evaluated for responses. The particle size of optimized formulation was found to be 271.18 nm that displayed zeta potential of –25.94 mV and EE of 68.16%. *In vitro* drug release study demonstrated 76.23% of CDR after 55 h. Formulation F_{10} was evaluated for surface morphology by transmission electron microscopy and the micrograph (Figure 5) revealed the spherical particles in the size range of 200 to 300 nm and few aggregates could also be observed.

The *in vitro* evaluated formulation F_{10} was subjected to pharmacokinetic and biodistribution studies. One of the most suitable methods of studying the biodistribution and pharmacokinetics of nanoparticles is to label these with radioisotopes like Tc-99m and to measure the biodistribution of radioactivity in various tissues following administration. Labeling efficiency of simvastatin SLNs and simvastatin suspension was measured and it was found that initially Tc-99m with both formulations shows >97.8% labeling efficiency. More than 94% labeling efficiency up to 48 h indicates the stability of radiolabeled complex (Table 3).

Following administration of the Tc-99m-labeled simvastatin suspension and simvastatin SLNs (F_{10}), the blood samples collected at various time intervals and analyzed for % A/G. % A/G versus time profile is shown in Figure 6. The data were used to calculate pharmacokinetic parameters (Table 4). The AUC for F_{10} was found to be 8.31% A/G h^{-1} that was fold higher as compared with AUC of simvastatin suspension amounting to 3.77% A/G h^{-1}. This clearly indicated increased bioavailability of simvastatin from SLNs and the relative bioavailability of simvastatin SLNs calculated by Equation (10) was determined as 220%.

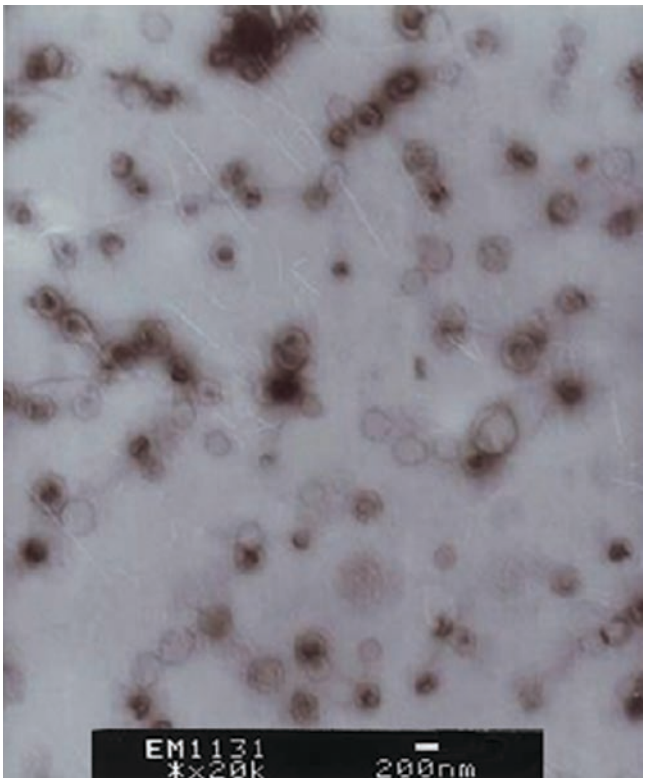

Figure 5. Transmission electron micrograph of the optimized solid lipid nanoparticle formulation F_{10} of simvastatin.

Table 3. Stability study data of radiolabeled complexes ($n = 3$).

	Normal saline		Mice serum	
Time (h)	Simvastatin suspension	Simvastatin SLNs	Simvastatin suspension	Simvastatin SLNs
0	96.87 ± 0.97	97.89 ± 1.07	98.39 ± 1.56	98.68 ± 1.22
0.5	98.34 ± 1.03	98.35 ± 0.79	98.11 ± 1.21	98.72 ± 1.08
1	97.67 ± 1.11	98.27 ± 1.09	97.86 ± 1.41	98.27 ± 1.17
2	98.84 ± 0.89	98.18 ± 0.98	97.42 ± 0.97	98.11 ± 1.04
4	98.45 ± 1.31	97.79 ± 1.16	97.25 ± 1.03	97.85 ± 1.14
6	98.08 ± 0.86	97.52 ± 1.06	97.16 ± 1.13	97.57 ± 1.08
24	97.11 ± 1.04	97.05 ± 1.21	96.89 ± 1.09	96.06 ± 0.87
48	95.09 ± 0.88	94.37 ± 1.18	94.38 ± 0.89	94.24 ± 1.95

$$\text{Relative bio availability} = \{AUC_{SLNs}/AUC_{suspension}\} \times 100 \quad (10)$$

where $AUC_{suspension}$ is the area under the curve for simvastatin suspension and AUC_{SLNs} is the area under the curve for simvastatin SLNs (F_{10}).

The increase in bioavailability of simvastatin from SLNs was due to minimized hepatic first-pass metabolism of simvastatin. It is suggested that the transport of drugs through the intestinal lymphatics via the thoracic lymph duct to the systemic circulation at the junction of the jugular and left subclavian vein avoids presystemic hepatic metabolism and therefore enhances

bioavailability. Lipids can enhance lymph formation and simultaneously promote lymph flow rate (Suresh et al., 2007) thereby affording protection against hepatic metabolism. Increased stability of simvastatin as SLNs to hydrolytic degradation in GI tract (Vanderbast et al., 2007) might be another reason for increasing bioavailability as acidic/alkaline condition of GI tract hydrolyzes lactone form of simvastatin to its hydroxyl acid derivative. Upon analysis of pharmacokinetic parameters, the elimination half-life of simvastatin from SLNs was found to be 3.13 times higher than from suspension due to the sustained release of drug from lipid nanoparticles that also resulted in reduced rate of absorption. An increase in V_d of simvastatin SLNs was demonstrable of wider tissue distribution as compared with simvastatin suspension that was confirmed by biodistribution studies.

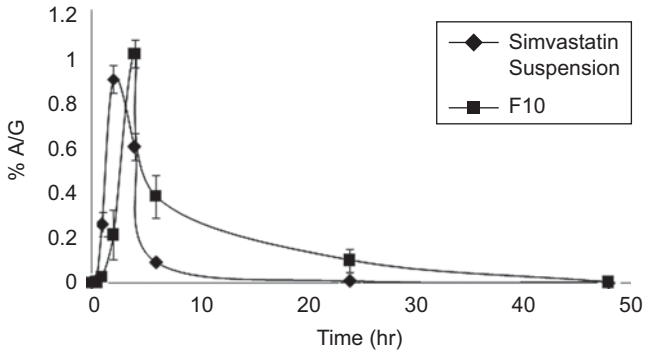

Figure 6. Percent activity per gram versus time profile of radiolabeled simvastatin suspension (—◆—) and formulation F_{10} (—■—) in blood after oral administration to mice ($n=3$).

Table 4. Pharmacokinetic parameters of simvastatin suspension and optimized formulation F_{10} after oral administration to mice ($n=3$).

Parameter	Simvastatin suspension	F10
Elimination half-life (h)	3.441	10.78
Absorption constant (h^{-1})	0.193	0.078
Elimination constants (h^{-1})	0.201	0.064
Volume of distribution (% radioactivity)	6.590	9.365
Clearance (h)	1.332	0.602
Area under curve (% A/G/h)	3.775	8.312
Relative bioavailability (%)	100	220

The biodistribution of Tc-99m-labeled formulations in heart, lungs, liver, spleen, kidney, stomach, and intestine was studied. Organ distribution of simvastatin in lungs, heart, spleen, and kidney was higher from SLNs as compared with suspension as shown in Table 5. The higher distribution was because of the long circulating time of drug in the blood, which led to more partition of drug in these tissues due to its high partition coefficient value. Simvastatin was highly distributed to lungs and spleen, which might be because of the higher perfusion rate of these organs than other.

Specifically, Figure 7A shows the distribution of drug in the stomach following oral administration of F_{10} and simvastatin suspension with respect to time. Initially, higher radioactivity was observed in stomach within 2 h of administration and predictively after 2 h the radioactivity in the stomach decreased because of the short gastric transit time of suspension and nanoparticulate formulation in the stomach. At the end of 24 h, trace amounts of simvastatin were observed from F_{10} and simvastatin suspension.

As the suspensions have short gastric residence time, it rapidly enters into the intestine. This was proved by the radioactivity measurements of intestine (Figure 7B). Maximum activity was observed at the second hour and at each time point the activity of simvastatin suspension was significantly less than F_{10} and was not observed beyond 24 h but activity of F_{10} was seen even at 48th hour. This may be attributed to the protective effect of SLNs against hepatic metabolism and also to the villae present in the intestine, in which nanoparticles can be easily entrapped for longer period of time.

Figure 7C shows comparative distribution of simvastatin in liver. It was observed that simvastatin from SLNs was poorly accumulated in the liver as compared with simvastatin from suspension within 2 h of administration. This was because of the lymphatic uptake of SLNs. The lymphatic

Table 5. Percent A/G versus time data of various organs of mice ($n=3$) after oral administration of simvastatin suspension and optimized solid lipid nanoparticle formulation F_{10}.

		% A/G at various time (h)						
Organ	Formulation	0.5	1	2	4	6	24	48
Heart	F_{10}	0.002 ± 0.00	0.018 ± 0.01	0.179 ± 0.04	0.480 ± 0.07	0.276 ± 0.03	0.061 ± 0.02	0.012 ± 0.01
	Simvastatin suspension	0.002 ± 0.00	0.0561 ± 0.01	0.164 ± 0.04	0.260 ± 0.07	0.071 ± 0.03	0.0056 ± 0.01	—
Lungs	F_{10}	—	0.021 ± 0.01	0.189 ± 0.04	0.689 ± 0.09	0.257 ± 0.09	0.074 ± 0.09	0.0089 ± 0.00
	Simvastatin suspension	—	0.099 ± 0.02	0.320 ± 0.05	0.378 ± 0.08	0.072 ± 0.01	0.0045 ± 0.03	—
Kidney	F_{10}	—	0.0342 ± 0.01	0.190 ± 0.03	0.308 ± 0.04	0.144 ± 0.06	0.083 ± 0.01	0.040 ± 0.01
	Simvastatin suspension	—	0.051 ± 0.03	0.080 ± 0.06	0.165 ± 0.06	0.0473 ± 0.01	0.0072 ± 0.00	—
Spleen	F_{10}	0.456 ± 0.09	0.756 ± 0.11	0.852 ± 0.22	0.396 ± 0.09	0.2000 ± 0.02	0.110 ± 0.09	0.0563 ± 0.02
	Simvastatin suspension	1.130 ± 0.40	1.590 ± 0.20	1.820 ± 0.30	0.231 ± 0.09	0.128 ± 0.09	0.0078 ± 0.00	—

—: Not measurable.

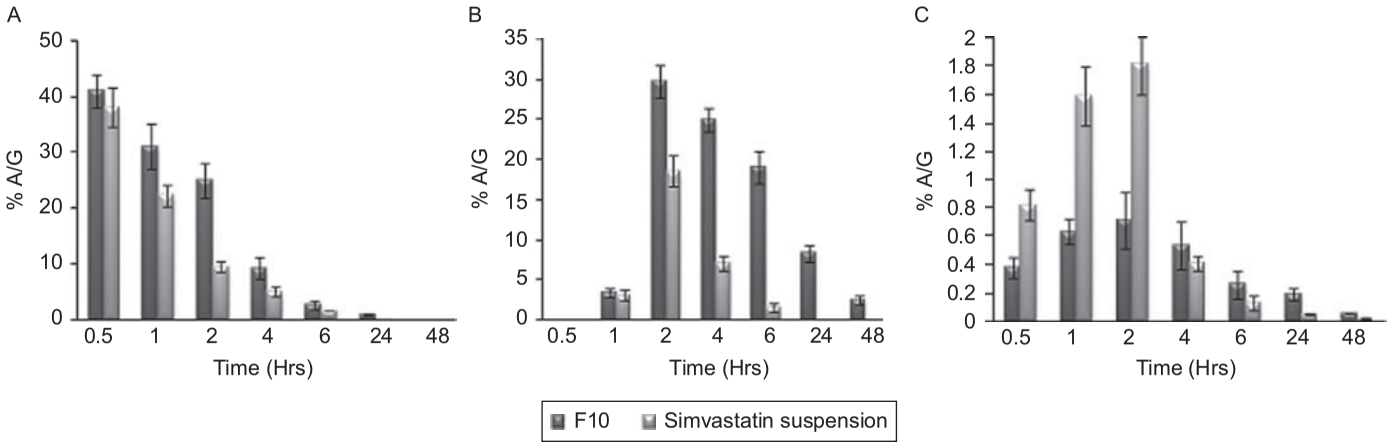

Figure 7. Percent activity per gram versus time histograms for simvastatin suspension (■) and formulation F_{10} (■) in (A) stomach, (B) small intestine, and (C) liver after oral administration to mice ($n = 3$).

transport of simvastatin incorporated into SLNs can be attributed to two possible mechanisms. First, exogenously administered triglycerides are digested by the action of pancreatic lipase/colipase digestive enzymes present in the small intestine and absorbed into enterocytes. After absorption, long-chain fatty acids or lipids are biosynthesized into triglyceride-rich lipoprotein particles (chylomicrons), which are secreted into intestinal lymph. The size of intestinal lipoproteins precludes their absorption into the blood capillaries and therefore they are secreted into the lymph. Second, cellular lining of the GI tract is composed of absorptive enterocytes interspersed with membranous epithelial (M) cells. M cells that cover lymphoid aggregates, known as Peyer's patches, take up nanoparticles by a combination of endocytosis or transcytosis.

It was shown that even after 2 to 4 h of administration, simvastatin from SLNs continuously entered into the liver. This is advantageous because the liver is the target organ to reduce the cholesterol level in blood. Transport of simvastatin from blood to liver is proposed to occur mainly via a Na^+-independent anion transporter in the sinusoidal membrane by passive diffusion (Nezasa et al., 2002). In liver, simvastatin is hydrolyzed into its active hydroxyl acid derivative and is acted upon the HMG coenzyme A reductase enzyme present in the liver and thus inhibiting the cholesterol synthesis. It is reported that despite the inhibition of HMG coenzyme A reductase hepatic cholesterol level does not fall. This is because hepatocytes compensate any drop in cholesterol level by increasing the synthesis of LDL receptor protein along with HMG CoA reductase. Because the newly synthesized HMG CoA reductase is inhibited too, the hepatocytes must meet its cholesterol demand by uptake of LDL from the blood and finally removing cholesterol from blood (Goodman and Gilman's, 2006). Simvastatin from prepared formulation (SLN) continuously entered the liver and expressed its therapeutic activity by proposed manner and thus has potential to lower blood cholesterol level for prolonged period.

Conclusion

Solid compritol nanoparticles of simvastatin were optimized and identified as preferred drug carrier to overcome first-pass metabolism of this lipophilic drug, thereby enhancing its oral bioavailability. The study demonstrated significant absorption of simvastatin incorporated in SLN with detectable plasma level achieved for several hours and the effect of nanoparticulate system on the biodistribution. Conclusively, SLN of simvastatin can enable improvement of drug bioavailability and reduction of the dosing frequency and may resolve the problem of nonadherence to prescribed therapy.

Acknowledgement

Authors are highly thankful to All India Council of Technical Education, New Delhi, India for providing financial support.

Declaration of interest

The authors report no declarations of interest.

References

Ali H, Shirode AB, Sylvester PW, Nazzal S. (2010). Preparation, characterization, and anticancer effects of simvastatin–tocotrienol lipid nanoparticles. Int J Pharm, 389, 223–231.

Almeida AJ, Runge S, Muller RH. (1997). Peptide-loaded solid lipid nanoparticles: influence of production parameters. Int J Pharm, 149, 255–265.

Babbar AK, Kashyap R, Chauhan UP. (1991). A convenient method for the preparation of 99mTc-labelled pentavalent DMSA and its evaluation as a tumor imaging agent. J Nucl Bio Med, 35, 100–104.

Bhavsar MD, Tiwari SB, Amiji MM. (2006). Formulation optimization for the nanoparticles-in-microsphere hybrid oral delivery system using factorial design. J Control Release, 110, 422–430.

Bolton S, Bon C. (2004). Pharmaceutical Statistics: Practical and Clinical Application, 4th ed. New York: Marcel Dekker.

Derakhshandeh K, Erfan M, Dadashzadeh S. (2007). Encapsulation of 9-nitrocamptothecin, a novel anticancer drug, in biodegradable nanoparticles: factorial design, characterization and release kinetics. Eur J Pharm Biopharm, 66, 34–41.

Freitas C, Muller RH. (1998). Effect of light and temperature on zeta potential and physical stability in solid lipid nanoparticle dispersions. Int J Pharm, 168, 221–229.

Goodman, and Gilman's (2006). The Pharmacological basis of Therapeutics, 10th ed. Hardman JG, Limbird LE, Eds. New York: McGraw-Hill.

Leroux JC, Allemann E, Doelker E, Gurny R. (1994). New approach for the preparation of nanoparticles by an emulsification-diffusion method. Eur J Pharm Biopharm, 41, 14–18.

Maaßen S, Schwarz C, Mehnert W, Lucks JS, Yunis-Specht F, Muller BW, Muller RH. (1993). Comparison of cytotoxicity between polyester nanoparticles and solid lipid nanoparticles. Proc Int Symp Control Rel Bioact Mater, 20, 490–491.

Manjunath K, Reddy JS, Venkateswarlu V. (2005). Solid lipid nanoparticles as drug delivery systems. Methods Find Exp Clin Pharmacol, 27, 127–144.

Margulis-Goshen K, Magdassi S. (2009). Formation of simvastatin nanoparticles from microemulsion. Nanomedicine, 5, 274–281.

Mehnert W, Mäder K. (2001). Solid lipid nanoparticles: production, characterization and applications. Adv Drug Deliv Rev, 47, 165–196.

Mishra P, Babbar A, Chauhan UP. (1991). A rapid instant thin layer chromatographic procedure for determining radiochemical purity of 99Tcm-IDA agents. Nucl Med Commun, 12, 467–469.

Mukherjee S, Ray S, Thakur RS. (2007). The current status of solid lipid nanoparticles. Pharmbit, XV, 53–60.

Muller RH, Maaßen S, Weyhers H, Specht F, Lucks JS. (1996). Cytotoxicity of magnetite loaded polylactide, polylactide/glycolide particles and solid lipid nanoparticles. Int J Pharm, 138, 85–94.

Müller RH, Mäder K, Gohla S. (2000). Solid lipid nanoparticles (SLN) for controlled drug delivery—a review of the state of the art. Eur J Pharm Biopharm, 50, 161–177.

Nastruzzi C. (2005). Lipospheres in Drug Targets and Delivery. New York: CRC Press.

Nezasa K, Higaki K, Matsumura T, Inazawa K, Hasegawa H, Nakano M, Koike M. (2002). Liver-specific distribution of rosuvastatin in rats: comparison with pravastatin and simvastatin. Drug Metab Dispos, 30, 1158–1163.

Nishioka Y, Yoshino H. (2001). Lymphatic targeting with nanoparticulate system. Adv Drug Deliv Rev, 47, 55–64.

Schubert MA, Müller-Goymann CC. (2003). Solvent injection as a new approach for manufacturing lipid nanoparticles—evaluation of the method and process parameters. Eur J Pharm Biopharm, 55, 125–131.

Shah M, Pathak K. (2010). Development and statistical optimization of solid lipid nanoparticles of simvastatin by using 23 full factorial design. AAPS Pharm Sci Tech, [online 23 March 2010%%Ea.

Suresh G, Manjunath K, Venkateswarlu V, Satyanarayana V. (2007). Preparation, characterization, and in vitro and in vivo evaluation of lovastatin solid lipid nanoparticles. AAPS PharmSciTech, 8, 24.

Theobald AE. (1990). Textbook of Radiopharmacy: Theory and Practice. Sampson CB, Ed. Gordon and Breach New York.

Vanderbast F, Sereno A, Bauduer P. (2007). Oral pharmaceutical composition containing a statin derivative. US Patent 4667088.

Yang S, Zhu J, Lu Y, Liang B, Yang C. (1999). Body distribution of camptothecin solid lipid nanoparticles after oral administration. Pharm Res, 16, 751–757.

Zhang D, Tan T, Gao L. (2003). Preparation of oridonin-loaded solid lipid nanoparticles and studies on them in vitro and in vivo. Nanotechnology, 17, 5821–5828.